

# **INFLUENCE OF THE OPERATING VARIABLES OF THE PRESS POWDER FEED SYSTEM ON BULK DENSITY DISTRIBUTION**

**J.M. Tiscar<sup>1</sup>, J. Boix<sup>1</sup>, G. Mallol<sup>1</sup>, J. Montolio<sup>1</sup>, L. Foucard<sup>1</sup>,  
R. Bonaque<sup>2</sup>, J.A. Pérez<sup>2</sup>**

**<sup>1</sup>Instituto de Tecnología Cerámica (ITC). Asociación de Investigación de las Industrias Cerámicas (AICE).**

**Universitat Jaume I. Castellón. Spain.**

**<sup>2</sup>MACER S.L**

## **1. ABSTRACT**

The filling of die cavities during the body forming stage is a critical step in the ceramic tile manufacturing process, which decisively affects the characteristics of the final product. This study systematically analyses, for the first time, the effect of feed system operating variables on powder distribution in the die cavities. The experiments were carried out on a test bench that enabled evaluation of the effect of the operating variables on bulk density distribution, the thickness and mass of the powder bed in a cavity of 30 cm x 60 cm and variable depth. The bulk density distribution and mass of the spray-dried powder bed deposited in the cavity was analysed using non-destructive X-ray absorption.

## 2. INTRODUCTION

The system used to feed spray-dried powder into the die cavities is one of the elements of the pressing facility that has developed least in recent decades. Although the presses designed to shape bodies have undergone considerable development, which has made it possible to go from the old friction presses to the current hydraulic presses in only 30 years, the powder feed system has, at present, the same conceptual design as those used in the 1970s [1].

In its simplest version, the powder feed system (see Figure 1) is composed, on the one hand, of a dosing hopper (traditionally fixed) that has been progressively replaced in recent years by a mobile dispenser, as the size of the manufactured pieces has increased. On the other hand, the transport system consists of a metal grid. The grid may have different geometric shapes, depending on the manufacturer and/or on user requirements. This feed system thus allows the spray-dried powder deposited previously in the dispenser to be transported to the openings in the die, by the longitudinal movement of the grid over the die.

During each filling cycle, the front part of the grid deposits the bodies formed in the previous pressing cycle onto the roller belt located at the press exit. At the same time, the powder necessary to form the following bodies falls into the die cavities, at the moment that the corresponding openings are formed, as a result of the displacement of the lower press punches to the first drop position. In its return movement to the charging position, the grid levels flush the powder deposited in the cavities, leaving the powder bed surface ready to receive the corresponding axial compression force. Once the compaction cycle has ended, the rise of the lower punches allows the shaped pieces to be extracted from the die, which are again pushed by the feeding system, thus initiating a new pressing cycle.



**Figure 1.** Spray-dried powder feed system used in industrial presses for forming ceramic tile bodies.

Heterogeneous powder distribution during the filling of the cavity leads to density differences in the resulting bed, which give rise to differences in bulk density of the shaped piece. Subsequently, during firing, if these differences are excessive, defects due to departures from rectangularity or so-called wedging frequently occurs [2].

Historically, lack of homogeneity in powder distribution has been offset by placing small metal sheets between the punches and the crosspiece that holds them, which redistribute the pressure within the piece in order to compensate for charge differences. More recently, isostatic punches have appeared on the market, which contain an oil bed between the polymer coating of the punch and the metal plate that constitutes the actual punch. This oil chamber enables redistribution of the pressure on the powder bed, without the need to add metal supplements, to obtain homogeneous bulk density distribution within each body.

The solutions proposed to solve the problems associated with poor powder distribution inside the press cavities do not directly affect powder distribution in the die. All solutions proposed so far have a passive character, on compensating charge deficiencies by redistributing the pressure applied to the powder bed. This approach is not wholly satisfactory given that problems of wedging continue to appear at the industrial level.

In order to solve this problem, simulation of die filling using the discrete element method (DEM) [3] has also been proposed as a promising alternative in studying how operating variables affect powder distribution in the cavities. Using this type of simulation, it is possible to directly study the microstructure of the powder deposited in the die, without the need for experimentation [4,5]. However, the computational cost of this methodology is quite high, thus for the moment not enabling quantitative results to be obtained. However, the wealth of qualitative information provided by these simulation tools, together with other characterization tools such as non-destructive analysis by X-ray absorption, open the doors to systematized optimal design of new powder feed systems.

### **3. OBJECTIVE**

The main objective of the study was to determine the effect of the different operating variables of the die filling process on the properties of the resulting powder bed. The effect of the following operating variables was studied: grid speed, moment of lower punch drop and charge thickness.

## **4. MATERIALS AND EXPERIMENTATION PROCEDURE**

### **4.1. MATERIALS AND EQUIPMENT**

In this study, a spray-dried powder commonly used in the manufacture of glazed porcelain stoneware tiles was used. Particle size distribution was fitted to a logarithmic normal distribution with a geometric mean ( $\mu_{geo}$ ) of 300  $\mu\text{m}$  and a geometric standard deviation ( $\sigma_{geo}$ ) of 1.43. Figure 2 shows the size distribution of the powder granules used. The powder used was dry in order to eliminate the effect of moisture on the results obtained.

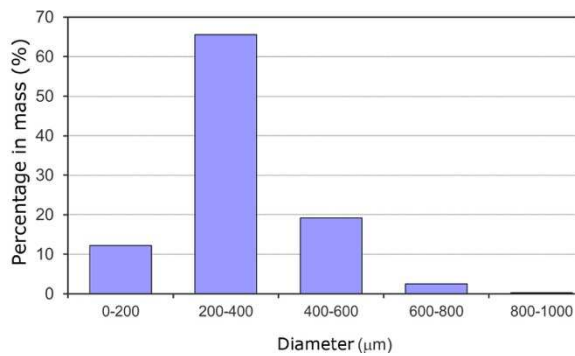


**Figure 2.** Size distribution of the spray-dried powder granules used in the process.

To study the influence of the operating variables on the die filling process, a pilot-scale powder feed system (Figure 3) was developed and constructed. In the constructed prototype, different elements are distinguished: a pre-hopper (1), feed hopper (2), exchangeable grid (3), die with a single cavity of 30 cm x 60 cm (4) and control system from which the movement of the different elements of the feed system (5) are programmed, as occurs in an industrial press.

To carry out a charge test, the spray-dried powder was placed inside the pre-hopper and then transferred to the lower hopper, manually removing the hatch that separated them. This reduced any potential operator influence on the distribution of the powder contained in the hopper.

Once the hopper was full, the grid-filling cycle began, according to a feed cycle programmed from the control system. The same grid-filling procedure was used for each test carried out in this study. First, the hopper moved to the front of the grid. The hopper hatch then automatically opened and drew back to its initial position, the powder being deposited on the grid. Once the grid had been completely filled, the charging cycle was carried out similarly to charging in an industrial press.



**Figure 3.** Pilot test bench for analysing die filling in ceramic tile manufacture.



**Figure 4.** Floating grids used in the study. Left: strip grid. Centre: grid with V-shaped scrapers. Right: honeycomb grid.

The influence of three different grid configurations on powder distribution in the cavity was studied: a floating grid with longitudinal strips, a floating grid with V-shaped scrapers (involving longitudinal strips that were thicker and wedge-shaped), and a floating grid of diagonally arranged square strips commonly known as a honeycomb grid (Figure 4). The term floating grid refers to grids mounted on a hermetically sealed frame, which rests on

the sliding plate of the die. These three designs correspond to the most common types of industrial grids used today.

## 4.2. X-RAY INSPECTION OF THE POWDER BEDS

To analyse the characteristics of the powder beds resulting from the charge tests carried out on the prototype, a non-destructive technique based on X-ray absorption was used. Thus, on ending each charge test, using a specially designed extraction system, the blades and the bottom of the cavity containing the deposited powder were extracted. The assembly formed was transferred to a DENSEXPLORER® (Figure 5) device that enabled measurement of the distribution of powder bed bulk density, thickness and mass [6].

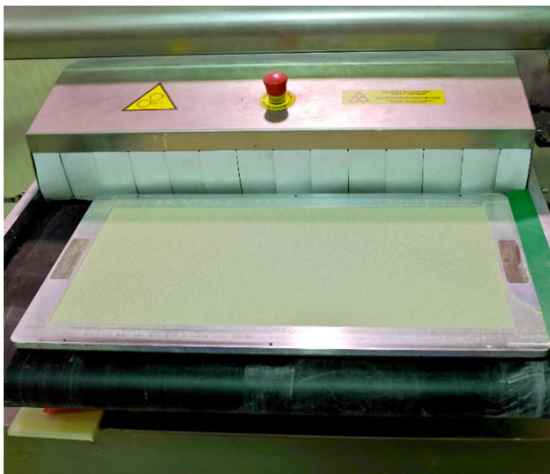


**Figure 5.** DENSEXPLORER® X-ray inspection device used to analyse the physical characteristics of powder beds.

The device directly measures the thickness and radiation absorption at each point on the surface of the material analysed, and then calculates bulk density while providing a map of bulk density distribution in false colour (Figure 6). The bulk density calculation is based on the Lambert-Beer law [7], and the device requires calibration prior to use.

The device was calibrated by analysing several powder beds of different thickness prepared with the same spray-dried powder used for the charge tests. Since the powder beds resulting from the tests carried out on the prototype were deposited onto the metal bottom of the cavity, the powder beds used in the calibration were also prepared on the same material. To this end, four cylindrical containers of different heights and the same metal base were made as the pilot cavity, and the powder was deposited inside it by free fall (Figure 7). The surface of each bed was carefully levelled flush with a spatula and its bulk density was determined based on its volume and the mass of powder used. By analysing the samples with the device, relationships between the attenuation capacity of the material, and bed thickness and density were obtained. This calibration relationship was used to determine the bulk density distribution maps of the different beds obtained with the prototype.

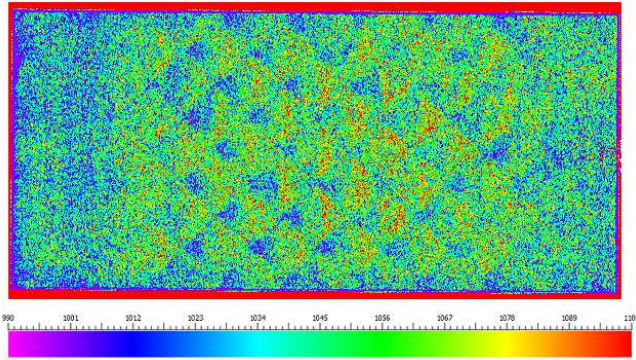


**Figure 6.** Bulk density ( $\text{kg/m}^3$ ) distribution map of a powder bed prepared with the prototype.



**Figure 7.** Test samples used for calibration of the X-ray device.

### 4.3. DESIGN OF EXPERIMENTS

In order to analyse the influence of the operating variables on powder distribution, a complete factorial design of experiments was previously carried out, covering all possible combinations among the operating variables studied.

Table 1 shows a summary of the operating variables examined and the corresponding levels of variation. These operating conditions were tested for the three test grid types. The moment of lower punch drop was defined as a percentage as a function of the relative position of the grid with respect to the beginning of the cavity. Thus, for example, a moment of drop at 0% means that the lower punch drop occurred at the same instant at which the front part of the grid coincided with the rear edge of the opening.

Operating variable	Ref	Level -	Level +
Grid speed (mm/s)	$V_p$	660	1320
Moment of lower punch drop (%)	$C_p$	60	90
Charge thickness (mm)	$E_{sp}$	13	18

**Table 1.** Operating variables and levels used in the design of experiments.

The variation limits of the variables were chosen to cover the range of variation customarily used in industrial conditions. A total of 24 filling experiments were carried out, modifying all the variables studied for the three types of test grids. After each filling test, the resulting powder bed was transferred to the X-ray inspection device and, based on the bulk density maps obtained, the average bulk density profiles through the cavity were determined. For all results corresponding to the density profiles shown in this study, the 600-mm distance corresponds to the front part of the cavity.

## 5. RESULTS AND DISCUSSION

### 5.1. HONEYCOMB GRID

First, the effects of the operating variables were analysed using the honeycomb grid. Figure 8 shows the average bulk density profiles corresponding to filling cycles obtained under the different testing conditions.

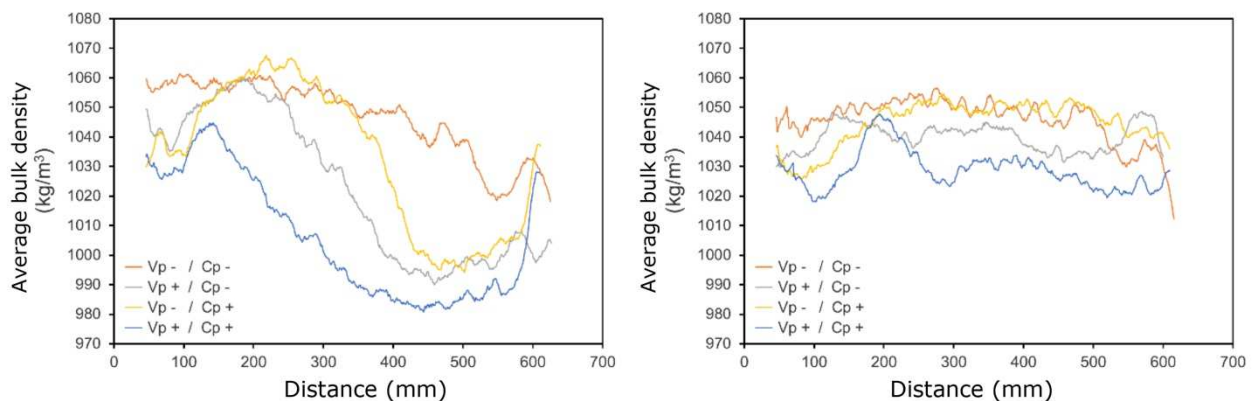


Figure 8. Average bulk density profiles corresponding to filling cycles using the honeycomb grid. Left: charge thickness of 13 mm. Right: charge thickness of 18 mm.

For a charge thickness of 13 mm (Figure 8, left), a lower bulk density was observed in the front part of the opening, regardless of the grid speed of advance or moment of lower punch drop. This behaviour, which may be due to the displacement of the powder produced by the grid during flush levelling of the bed, was more pronounced as grid speed of advance increased and the first punch drop was delayed. For this configuration, the most homogeneous bulk density distribution was achieved with a grid speed of 660 mm/s and a moment of lower punch drop at 60% (orange line). In addition, under these conditions the highest bulk density of the bed was achieved. In principle, in industrial practice, filling cycles that provide bed densities as high as possible are preferable, since, the amount of air to be removed during the de-airing cycle will be less. This will have a favourable effect on the quality of the product as well as the possibility of shortening the duration of the pressing cycles.

With respect to the experiments carried out for a charge thickness of 18 mm (Figure 8, right), the bulk density values were more homogeneous in all cases with respect to those of the 13-mm charge. As in the previous configuration, the highest and most homogeneous density was achieved when the grid speed was 660 mm/s and the moment of lower punch drop was 60%. It should be noted that, unlike charge thicknesses of 13 mm, at 18 mm the differences observed between density profiles were much less significant. In addition, the effect of the moment of punch drop was less notable, the effect of grid speed of advance being more important for the resulting density distribution. This fact shows that distortions caused by the flush levelling of the powder during grid return had a lower incidence as bed thickness increased.

## 5.2. STRIP GRID

Figure 9 shows the average bulk density profiles corresponding to the filling tests carried out using the strip grid. With respect to the cases corresponding to a charge thickness of 13 mm (Figure 9, left), two different trends may be observed. On the one hand, the results corresponding to low grid speeds showed higher bulk densities, although with a significant decrease in density at the front part of the cavity, this being less pronounced with earlier punch drops. The results corresponding to high speeds show the same pattern of behaviour, but the differences between the front and rear of the opening were more pronounced. This behaviour was analogous to that observed for the same charge thickness for the honeycomb grid, although in this case the difference between different speed cycles was more significant. In fact, in the case of the honeycomb grid, the area of lower bulk density observed in the front of the opening was reduced more notably on decreasing grid speed and advancing punch drop.

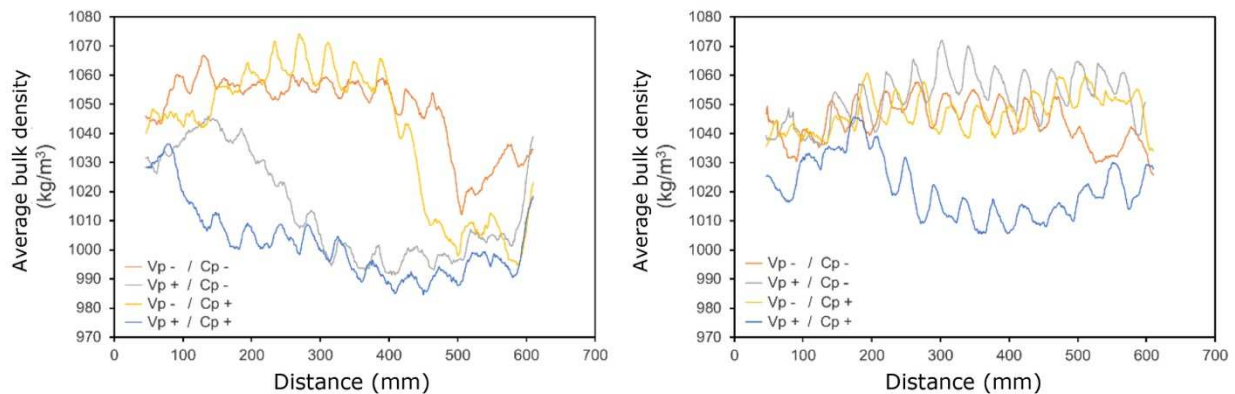


**Figure 9.** Average bulk density profiles corresponding to filling cycles using the strip grid. Left: charge thickness of 13 mm. Right: charge thickness of 18 mm.

As regards filling cycles with charge thicknesses of 18 mm (Figure 9, right), these all led to higher and more homogeneous bulk density, except for the cycle corresponding to high grid speeds and lower punch drop moment. Under these specific conditions, bulk density values were significantly lower and heterogeneous. To be noted was filling carried out at a high grid speed with the moment of lower punch drop at 60% (yellow line), whose density profile was highly acceptable for filling carried out at high grid speed.

Unlike that observed with the honeycomb grid, in this case for charge thicknesses of 18 mm, the moment of punch drop did affect powder distribution. In fact, at high advance speed, when punch drop was delayed (bluish line), the density at the front of the cavity was reduced by approximately  $50 \text{ kg/m}^3$  with respect to the other conditions. These results indicate that, with respect to the honeycomb grid, the strip grid exerted a greater distortion on density distribution during flush levelling of the powder bed.

Finally, it is interesting to note that the bulk density profiles provided by the honeycomb grid exhibited fewer swings than those obtained with the strip grid. In fact, the analysis of profiles corresponding to the strip grid shows that the separation observed during periodic swings in density distribution was of an order of magnitude similar to the gap existing between the strips. This may be due to the fact that the strip grid caused small local segregations of the spray-dried powder granules around the

separating sheets, which resulted in variations in density of the powder bed once deposited. The fact that no notable swings were observed in the honeycomb grid does not mean that there were no density variations due to the effect of the grid (Figure 6). The reason why they are not observed in the profiles is that they have been averaged along the axis perpendicular to the filling direction. The behaviour observed explains why, on an industrial level, aesthetic defects in the final product occasionally occur with respect to marking, at the face of the product, from the shape of the grid used in the feeder.

### 5.3. GRID WITH V-SHAPED SCRAPERS

Figure 10 shows the bulk density profiles corresponding to filling cycles carried out using the grid with V-shaped scrapers. The cycles corresponding to a charge thickness of 13 mm (Figure 10, left) exhibit the same behaviour as that observed with the previous grids, although the overall density values reached in each cycle were slightly lower. As with the two previous grids, this behaviour was associated with the distortion caused during flush levelling of the bed, whose effect on the density profiles obtained was greater as charge thickness decreased.

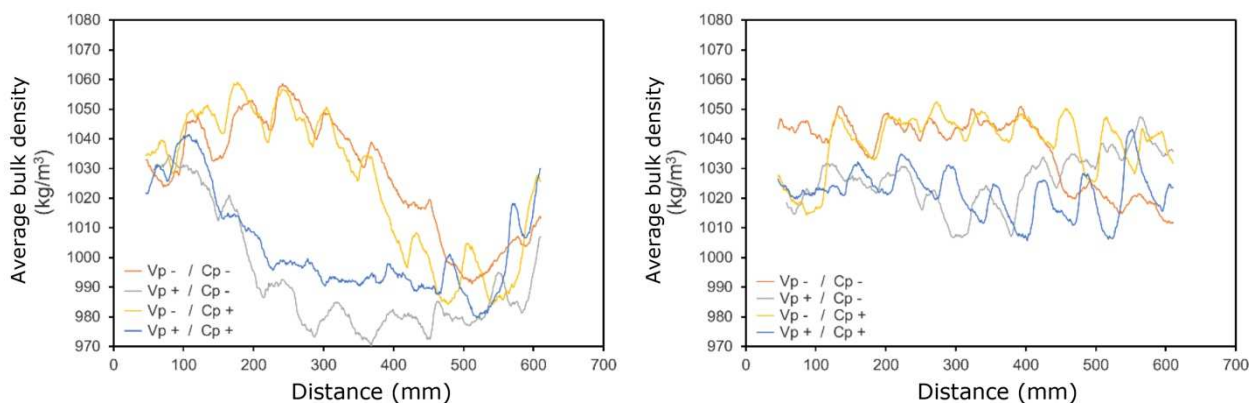


**Figure 10.** Average bulk density profiles corresponding to filling cycles using the grid with V-shaped scrapers. Left: charge thickness of 13 mm. Right: charge thickness of 18 mm.

With respect to the cycles corresponding to a charge thickness of 18 mm (Figure 10 **figure 10**, right), the bulk density values obtained were still lower than for the previous grids, although there remained a general trend to obtaining higher bulk density values along with greater homogeneity as feed system speed decreased. At the same time, as in the case of the strip grid, for cycles with a high grid speed, a lower punch drop at 60% led to higher density at the front of the die, with respect to a drop at 90%.

Finally, as in the previous case, the bulk density profiles displayed periodic swings due to the shape of the scrapers. In this case, the swings were more pronounced than in the previous case, as a result of the greater thickness of the scrapers with respect to that of the metal strips.

### 5.4. BULK DENSITY MAPS. COMPARATIVE ANALYSIS

Finally, by way of example, Figure 11 shows the bulk density maps corresponding to the powder beds obtained using the three types of grids (rows), with the filling cycles that led to a charge thickness of 18 mm and a moment of lower punch drop at 90%. These conditions provided better bulk density distribution compared to cycles with a charge thickness of 13 mm. The conditions of slower ( $V_{p-}$ ) (left column) and faster ( $V_{p+}$ ) (right column) grid speeds have also been included. The numerical values shown on the bulk density maps correspond to the average bulk density values for each of the rectangles into which the images have been divided.

1030	1044	1050	1052	1047	1046	1031	1042	1032	1031	1031	1027
1024	1044	1051	1051	1054	1045	1029	1041	1035	1035	1030	1028
1029	1077	1055	1052	1051	1047	1032	1042	1035	1036	1032	1026
1031	1040	1050	1053	1055	1046	1026	1036	1032	1034	1032	1023
1035	1048	1055	1049	1052	1040	1027	1039	1032	1037	1028	1026
1036	1044	1049	1048	1045	1039	1028	1035	1031	1031	1028	1024

1041	1050	1047	1049	1051	1055	1026	1039	1021	1013	1017	1028
1042	1050	1051	1047	1052	1055	1029	1046	1023	1018	1018	1026
1043	1049	1054	1045	1050	1054	1035	1045	1024	1019	1019	1026
1043	1047	1052	1047	1048	1053	1031	1041	1026	1021	1019	1024
1039	1050	1050	1048	1050	1053	1028	1038	1026	1019	1020	1024
1033	1038	1043	1041	1054	1052	1020	1029	1021	1013	1017	1024

1024	1040	1045	1048	1040	1041	1027	1026	1026	1022	1027	1030
1026	1043	1046	1045	1039	1043	1029	1029	1028	1020	1024	1029
1028	1044	1046	1046	1040	1042	1028	1032	1031	1018	1023	1025
1028	1045	1046	1044	1038	1042	1029	1032	1029	1017	1020	1023
1026	1042	1046	1043	1038	1040	1025	1031	1032	1018	1023	1022
1024	1040	1049	1047	1039	1036	1022	1022	1029	1020	1026	1025

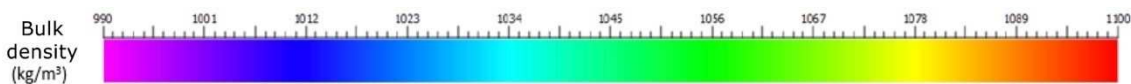


**Figure 11.** Bulk density maps corresponding to the cycles tested with a charge thickness of 18 mm and moment of lower punch drop at 90%. Left column:  $V_{p-}$ . Right column:  $V_{p+}$ . Top: Honeycomb grid. Centre: Strip grid. Bottom: Grid with V-shaped scrapers.

As has been demonstrated on analysing the average bulk density profiles, in all cases grid shape was reflected in the bulk density maps. On the other hand, increasing grid speed resulted in lower bulk density in all cases, regardless of the type of grid used. Nevertheless, the honeycomb grid proved to be the most robust grid, being less susceptible to potential changes in the different variables studied in this paper.

Finally, the symmetrical character of the filling with respect to a transverse axis was demonstrated, given that the main variations in bulk density occurred along the longitudinal axis of the die.

## 6. CONCLUSIONS

The experiments carried out show the different effects that the operating variables studied for die filling have on the characteristics of the powder bed deposited in the cavities and, therefore, on the quality of the final product. The conclusions of this study are detailed below:

- Charge thickness has a decisive influence on the filling of the cavities. The greater the charge thickness, the more homogeneous the bulk density of the deposited bed, and the less influenced by other operating variables. However, this variable is determined by the final thickness of the piece to be obtained.
- Grid speed directly affects the final density profile obtained. The greater the grid speed, the lower the bulk density of the deposited bed and the greater the heterogeneity of the resulting density profile.
- The moment of lower punch drop has less influence on filling homogeneity than grid speed. Its effect is important when modifying the bulk density of the front part of the powder bed, especially when grid speed is high and strip grids and grids with V-shaped scrapers are used.
- The geometric configuration of the grid has a significant effect on the distribution of the deposited powder. The greater the charge thickness, the greater the effect of the shape of the grid on the distribution of the powder bed. Finally, the thinner the grids, the fewer bulk density swings occur in the cavity.

## 7. ACKNOWLEDGEMENTS

The authors of this paper would like to thank the Centro para el Desarrollo Tecnológico Industrial (CDTI) and the Instituto Valenciano de Competitividad Empresarial (IVACE) for the economic support provided to conduct the study.

## 8. REFERENCES

- [1] R. Galindo Renau, *Prensas, moldes y prensado en la fabricación de baldosas cerámicas*, Macer, 2008.
- [2] J.. Amorós, V. Beltrán, A. Blasco, J.. Enrique, A. Escardino, *Defectos de fabricación de pavimentos y revestimientos cerámicos*, Valencia, 1991.
- [3] N. Bell, Y. Yu, P.J. Mucha, *Particle-based simulation of granular materials*, Proc. 2005 ACM SIGGRAPH/Eurographics Symp. Comput. Animat.
- [4] J.. Tiscar, A. Escrig, A. Pascual, F.A. Gilabert, R. Bonaque, J.A. López, *Análisis de la operación de llenado del molde durante el proceso de prensado de baldosas cerámicas.*, in: *World Congress on Ceramic Tile Quality*, Castellón, Spain, 2016.
- [5] J. Tiscar, A. Escrig, G. Mallol, J. Boix, F.A. Gilabert, *Influence of the die filling parameters during the ceramic tile pressing process via Discrete Element Method (DEM)*, en: *Shap. VI - Sixth Int. Conf. Shap. Adv. Ceram.*, Montpellier (France), 2016.
- [6] J.L. Amorós, J. Boix, D. Llorens, G. Mallol, I. Fuentes, C. Feliu, *Non-destructive measurement of bulk density distribution in large-sized ceramic tiles*, *J. Eur. Ceram. Soc.* 30 (2010) 2927-2936. doi:10.1016/j.jeurceramsoc.2010.01.033.
- [7] D.F. Swinehart, *The Beer-Lambert Law*, *J. Chem. Educ.* 39 (1962) 333.